

Radiation necrosis of the pons after radiotherapy for nasopharyngeal carcinoma: Diagnosis and treatment

Matthew N DeSalvo^{1*}

1. Harvard Medical School, Boston, MA, USA

* Correspondence: Matthew N DeSalvo, Harvard Medical School, 25 Shattuck Street, Boston, MA 02115, USA
(✉ matthew_desalvo@hms.harvard.edu)

Radiology Case. 2012 Jul; 6(7):9-16 :: DOI: 10.3941/jrcr.v6i7.1108

ABSTRACT

We report a case of radiation necrosis in an unusual location, the pons, in a patient who had received chemoradiation for nasopharyngeal carcinoma (NPC) over one year prior to presentation. This patient presented with subacute onset of ataxic hemiparesis and slurred speech. Initial magnetic resonance imaging (MRI) studies showed two 1-2cm peripherally contrast-enhancing lesions in the pons with extensive surrounding edema. Proton magnetic resonance spectroscopy (MRS) played a key role in narrowing the differential diagnosis to radiation necrosis. The patient underwent biweekly bevacizumab therapy and has remained clinically stable with radiologic improvement of his lesion. In addition to this case, we present an overview of the use of advanced neuroimaging in distinguishing radiation necrosis of the central nervous system (CNS) from other entities as well as the role of bevacizumab in treatment.

CASE REPORT

CASE REPORT

A 57-year-old Chinese man came to the emergency department due to one week of worsening slurred speech in the setting of gradually progressive left-sided weakness and incoordination. One month prior to presentation, he noticed that his left lower extremity felt heavy and that it "would not cooperate" during movement. One week later he developed a similar sensation in his left upper extremity which led to difficulty in performing fine motor tasks such as buttoning his shirt. One week prior to presentation he began to have a subjective sense of slurred speech. This set of symptoms occurred in the setting of having completed combination chemo-radiation therapy 14 months prior to presentation for NPC. Unfortunately, neither the specific chemotherapy regimen nor the radiotherapy dosing and shielding methods could not be obtained as the patient received treatment at an unknown foreign medical center. He was afebrile with vital signs within normal limits. Physical examination was notable for left-sided ataxic hemiparesis and was otherwise normal. Laboratory studies were unremarkable. A contrast MRI of the head revealed two well-circumscribed peripherally contrast-enhancing T1 hypointense lesions in the pons with extensive

surrounding fluid attenuated inversion recovery (FLAIR) edema and no evidence of recurrent NPC or mass effect (Fig. 1). A lumbar puncture showed normal cell counts and chemistry with no malignant cells on cytology. The differential diagnosis at this time included radiation necrosis, brainstem glioma, primary CNS lymphoma, toxoplasmosis and viral or listerial rhombencephalitis. A proton MRS study was ordered which revealed increased lactate and lipids with reduced neuroglial markers, consistent with the metabolic profile of radiation necrosis (Fig. 2). The diagnosis of radiation necrosis was made and aggressive treatment was initiated to prevent progression of the lesion and development of locked-in syndrome. The patient was started on 10mg/kg biweekly bevacizumab therapy and discharged from the hospital. His condition has remained stable as of 10 week post-discharge follow-up, and an MRI taken at that time showed decreased edema and reduced contrast enhancement (Fig. 3).

DISCUSSION

Radiation necrosis in the CNS is an uncommon serious adverse effect of radiotherapy that usually develops one to

three years after treatment. Necrosis following treatment of NPC is typically located in the deep white matter of the medial inferior temporal lobes, with relative cortical sparing. Radiation necrosis affects men and women equally and has been reported in up to 3% of all patients who receive cranial radiotherapy. The neurological deficits accompanying radiation necrosis depend on the anatomical regions affected and may present as either focal or generalized signs and symptoms. The pathophysiology of radiation necrosis is incompletely understood, but is thought to be a slowly evolving process involving vascular endothelial damage, fibrinoid necrosis, microscopic coagulation, demyelination and altered blood-brain barrier (BBB) permeability [1].

The initial MRI study of this patient revealed two well-circumscribed peripherally contrast-enhancing T1 hypointense lesions in the pons measuring 14 and 15 mm with diffuse FLAIR edema extending into the lower midbrain, upper medulla and right inferior cerebellar peduncle. Diffusion weighted imaging (DWI) showed no diffusion abnormality (Fig. 1). After obtaining this study, the differential diagnosis for this patient's lesions was broad and included infection, neoplasm and radiation necrosis. The use of advanced imaging modalities including MRS, MR perfusion, DWI, ¹⁸F-fluorodeoxyglucose positron emission tomography (¹⁸FDG-PET), ¹¹C-methionine (¹¹C-MET) PET, ²⁰¹thallium (Tl) single photon emission computed tomography (SPECT) and ¹²³I-methyltyrosine (¹²³IMT) SPECT can help distinguish necrosis from other entities. We will now review the relevant imaging findings of the diagnoses which remained on our differential after the initial MRI: radiation necrosis, brainstem glioma, primary CNS lymphoma, toxoplasmosis and listerial or viral rhombencephalitis.

Radiation-induced changes in the CNS typically are localized to the temporal lobes in patients treated for NPC. Lesions usually affect white matter more than gray matter and typically leave the cerebral cortex relatively spared. MRI of these lesions shows low T1 signal with high T2 signal that may extend beyond the irradiated tissue, representing cerebral edema. Lesions are typically round or irregular and have been described as "Swiss cheese" or "soap bubble" in appearance [2,3]. Contrast-enhancement patterns vary from small and nodular to ring-enhancing. DWI, although unrevealing in this case, typically shows elevated diffusion, which is a helpful distinction from cerebral abscesses and some tumors [4]. MRS, as in this case, shows a dominant lactate peak, with increased lipids, while other neuro-glial markers (choline, n-acetylaspartate (NAA), creatine) are typically reduced (Fig. 2) [4]. Perfusion studies typically show reduced cerebral blood volume in areas of necrosis [4]. ¹⁸FDG-PET usually shows hypometabolism, but reports of hypermetabolism exist. Finally, other nuclear studies such as ¹¹C-MET PET, ¹²³IMT SPECT and ²⁰¹Tl SPECT typically show reduced uptake in necrosis reflecting hypometabolism[5].

As in most cases where a suspicious intracranial lesion is detected in a patient who has undergone cranial radiation therapy, our main diagnostic question was to differentiate necrosis from neoplasm. We were particularly concerned about high-grade gliomas, as these tumors have MRI findings

similar to those of radiation necrosis. About 100 brainstem gliomas are diagnosed annually in the adult population in the United States. These tumors often arise at the cervicomedullary junction and infiltrate into descending pyramidal fibers or disrupt nearby cranial nerve nuclei. On MRI, they are often limited in size (<2cm) and may appear either cystic and well-demarcated, or more complex with exophytic growth, hemorrhage, necrosis and mass effect [6]. They are typically T1 hypointense or isointense and T2 hyperintense. Lower grade gliomas may be uniformly enhancing, while higher grade gliomas are more likely to show peripheral contrast enhancement [7]. Diffusion weighted imaging (DWI) often shows restricted diffusion due to altered white matter integrity with axonal disruption. However, conventional MRI and even DTI may not adequately differentiate necrosis from tumors, and other modalities are often more illustrative. MRS will show increased lactate if necrosis is present, with decreased n-acetylaspartate (NAA) and increased choline. In general, while neoplastic lesions tend to have increased cerebral blood volume as well as increased glucose and amino acid metabolism, necrotic lesions tend to have reduced perfusion and be hypometabolic as reflected through MR perfusion, ¹⁸FDG-PET, ¹¹C-MET PET and ¹²³IMT SPECT studies. ²⁰¹Tl SPECT, which reflects a combination of blood flow, BBB permeability and cellular uptake, typically shows increased uptake in gliomas compared to necrosis [6].

Primary lymphoma of the CNS is an overall uncommon entity, accounting for only 4% of all primary CNS tumors. It is typically associated with immunosuppression as in HIV/AIDS, iatrogenic immunosuppression or congenital immunodeficiency. It is extremely rare in the immunocompetent patient. Lesions of primary CNS lymphoma are usually solitary and have an affinity for the periventricular areas of the brain, with isolated brainstem involvement being extremely unusual [8]. Signal intensity on T1 and T2 MRI is usually hypo- or isointense, and contrast enhancement is typically uniform, with ring-enhancement being uncommon [8]. MRS and DWI profiles are similar to those described above for high-grade gliomas. Nuclear studies including ¹⁸FDG-PET, methionine PET, and ²⁰¹Tl or ^{99m}Tc (^{99m}Tc) SPECT all show increased uptake, reflecting the increased metabolic state of lymphoma tissue compared to normal brain parenchyma [9,10,11].

Cerebral toxoplasmosis, which is usually seen in patients who are immunocompromised secondary to HIV/AIDS, cancer or chemotherapy, targets the basal ganglia in up to 75% of cases. However, lesions in the brainstem are possible. Toxoplasmosis lesions are usually multiple and may cause mass effect. Their hallmark sign is the asymmetric target sign seen on MRI or computed tomography (CT), in which a ring-enhancing abscess contains smaller similarly-enhancing abscesses and eccentric nodules. The characteristics and enhancement patterns of toxoplasmosis on conventional MRI are otherwise similar to those of radiation necrosis. MRS in toxoplasmosis shows a similar profile to necrosis with elevated lactate and lipid peaks without neuroglial markers [12]. One important differentiating modality is DWI, which typically shows restriction in toxoplasmosis. Reduced uptake in nuclear

imaging studies such as ^{18}F FDG-PET, ^{201}Tl SPECT, $^{99\text{m}}\text{Tc}$ SPECT and sestamibi may be useful to distinguish toxoplasmosis from neoplasms, but larger prospective studies are required. In this case, our patient was not immunocompromised and had no exposure to or signs of infection with toxoplasmosis.

Listerial rhombencephalitis is a rare entity which has been described through case series as manifesting with a classic biphasic clinical course characterized by an early prodrome of fevers, headache, nausea and vomiting followed by progressive asymmetrical cranial nerve palsies, cerebellar signs, hemiparesis and loss of consciousness [13]. In case reports, MRI reveals patchy or peripheral contrast-enhancement and ill-defined T2 hyperintensity with hyperintensity on DWI sequences [14,15]. $^{99\text{m}}\text{Tc}$ SPECT shows decreased uptake which can last for up to 6 months although residual findings on MRI may be minimal [16]. Viral rhombencephalitis is also uncommon, but herpes simplex virus (HSV), Epstein-Barr virus, adenovirus, enterovirus 71, coxsackie virus and JC virus have been implicated in case reports as causative agents of rhombencephalitis [17,18,19]. On MRI, these lesions typically appear T1 hypointense and T2 hyperintense with irregular patterns of contrast enhancement. HSV rhombencephalitis has been described as having a leptomenigeal or gyriform pattern of contrast enhancement [17]. Again, because our patient had no biochemical or clinical signs of infection, and because these infections are so uncommon, they were much lower on our differential.

To summarize, our patient presented within the typical timeframe during which radiation necrosis following cranial radiotherapy would occur. Physical examination was notable for left ataxic hemiparesis, but was otherwise unrevealing. Imaging and MRS played an important role in localizing his lesion to the pons and establishing a diagnosis of radiation necrosis. Our patient was immediately started on bevacizumab, an anti-vascular endothelial growth factor (VEGF) monoclonal antibody, which has been recently shown to be effective treatment for radiation necrosis in the CNS.

Local hypoxia from endothelial cell damage leading to release of VEGF is thought to be important in the pathophysiology of alterations in BBB permeability, which provides a rationale for treatment with this relatively new therapy. The first case series of 8 patients with radiation necrosis in the CNS treated with bevacizumab (either 5 mg/kg every 2 weeks or 7.5 mg/kg every 3 weeks) showed reduction in dexamethasone dose and improvements on T1-weighted post-gadolinium and FLAIR MRI [20]. A retrospective review of 6 patients with biopsy-proven radiation necrosis treated with bevacizumab 10mg/kg every 2 weeks between 2006 and 2008 showed similar radiologic improvements [21]. In a randomized double-blinded trial with 14 patients with confirmed radiation necrosis, all patients in the treatment arm (7.5 mg/kg every 3 weeks, four cycles) experienced clinical improvement and at least partial radiologic resolution by MRI criteria while no patient who received placebo (saline) improved [22]. While these studies are encouraging, they are limited by small sample size and a follow-up time of no more than 10 months. It will be important to continue to study the

effects of bevacizumab in larger cohorts and for longer time periods to see if these clinical and radiologic improvements are robust and long-lasting.

Palliative efforts including surgical decompression and corticosteroids have been used historically to provide symptomatic relief and reduce cerebral edema associated with cerebral radiation necrosis. Other therapies including anticoagulation and hyperbaric oxygen have been reported in some cases to offer benefit, but there is little evidence to support their use.

In this case, our patient was aggressively treated with 10mg/kg biweekly bevacizumab to prevent the development of locked-in syndrome. As of 10 weeks after the initiation of therapy, he had not developed any new or worsening symptoms, though his left-sided ataxic hemiparesis remained. His MRI at that time showed reduced lesion volume with less contrast enhancement and edema, though it remains to be seen if his clinical course will improve, remain stable or worsen (Fig. 3).

TEACHING POINT

This report discusses the radiological findings of radiation necrosis seen on MRI including areas of T1 hypointensity with more extensive T2 hyperintensity and nodular or peripheral contrast enhancement. MRS typically shows increased lactate with reduced neuroglial markers, and this modality, along with nuclear imaging, can help distinguish radiation necrosis from other more metabolically active entities.

REFERENCES

1. Burger PC, Mahley MS Jr, Dudka L and Vogel FS. The morphologic effects of radiation administered therapeutically for intracranial gliomas: a postmortem study of 25 cases. *Cancer*. 1979;44(4):1256. PMID: 387205.
2. Van Tassel P, Bruner JM, Maor MH et al. MR of toxic effects of accelerated fractionation radiation therapy and carboplatin chemotherapy for malignant gliomas. *AJNR*. 1995 Apr;16(4):715-26. PMID: 7611028.
3. Kumar AJ, Leeds NE, Fuller GN et al. Malignant gliomas: MR imaging spectrum of radiation therapy- and chemotherapy-induced necrosis of the brain after treatment. *Radiology*. 2000 Nov;217(2):377-84. PMID: 11058631.
4. Offiah C and Hall E. Post-treatment imaging appearances in head and neck cancer patients. *Clin Radiol*. 2011 Jan;66(1):13-24. PMID: 21147294.
5. Chong VF, Fan YF and Mukherji SK. Radiation-induced temporal lobe changes: CT and MR imaging characteristics. *AJR*. 2000 Aug;175(2):431-6. PMID: 10915689.

6. Caroline I and Rosenthal MA. Imaging modalities in high-grade gliomas: Pseudoprogression, recurrence, or necrosis? *J Clin Neuroscience*. 2012 Feb 7. Epub ahead of printing. PMID: 22321359.
7. Barkovich AJ, Krischer J, Kun LE et al. Brain stem gliomas: a classification system based on magnetic resonance imaging. *Pediatr Neurosurg*. 1990-1991;16(2):73-83. PMID: 2132928.
8. Schwingel R, Reis F, Zanardi VA Quieroz LS and França MC Jr. Central nervous system lymphoma: magnetic resonance imaging features at presentation. *Arq Neuropsiquiatr*. 2012 Feb;70(2):97-101. PMID: 22311212.
9. Villringer K, Jäger H, Dichgans M et al. Differential diagnosis of CNS lesions in AIDS patients by FDG-PET. *J Comput Assist Tomogr*. 1995 Jul-Aug;19(4):532-6. PMID: 7622678.
10. Ogawa T, Kanno I, Hatazawa J et al. Methionine PET for follow-up of radiation therapy of primary lymphoma of the brain. *Radiographics*. 1994 Jan;14(1):101-10. PMID: 8128041.
11. De la Peña RC, Ketonen L and Villanueva-Meyer J. Imaging of brain tumors in AIDS patients by means of dual-isotope thallium-201 and technetium-99m sestamibi single-photon emission tomography. *Eur J Nucl Med*. 1998 Oct;25(10):1404-11. PMID: 9818280.
12. Simone IL, Federico F, Tortorella C et al. Localised 1H-MR spectroscopy for metabolic characterisation of diffuse and focal brain lesions in patients infected with HIV. *J Neurol Neurosurg Psychiatry*. 1998 Apr; 64(4):516-23. PMID: 9576546.
13. Armstrong RW and Fung PC. Brainstem encephalitis (rhombencephalitis) due to *Listeria monocytogenes*: case report and review. *Clin Infect Dis*. 1993;16(5):689. PMID: 8507761.
14. Alper G, Knepper L and Kanal E. MR findings in listerial rhombencephalitis. *AJNR*. 1996 Mar; 17(3):593-6. PMID: 8881261.
15. Benito-Leon J, Alvarez-Linera J, Jimenez L and Valera M. Diagnostic usefulness of diffusion-weighted magnetic resonance imaging in listerial rhombencephalitis. *Eur J Neurol*. 2002 Nov;9(6):693-4. PMID: 12453092.
16. Sahin S, Arisoy AS, Topkaya AE and Karsidag S. Brainstem listeriosis: a comparison of SPECT and MRI findings. *MedGenMed*. 2006;8(4):47. PMID: PMC1868329.
17. Zagardo MT, Shanholtz CB, Zoarski GH and Rothman MI. Rhombencephalitis caused by adenovirus: MR imaging appearance. *AJNR*. 1998 Nov. 19:1901-3. PMID: 9874544.
18. Goto K, Sanefuji M, Kushara K et al. Rhombencephalitis and coxsackievirus A16. *Emerg Infect Dis*. 2009 Oct. 15(10):1689-91. PMID: 19861078.
19. Moragas M, Martinez-Yelamos S, Majos C, Fernandez-Viladrich P, Rubio F and Arbizu T. Rhombencephalitis: a series of 97 patients. *Medicine (Baltimore)*. 2011 Jul;90(4):256-61. PMID: 21694648.
20. Gonzalez J, Kumar AJ, Conrad CA and Levin VA. Effect of bevacizumab on radiation necrosis of the brain. *Int J Radiat Oncol Biol Phys*. 2007; 67(2):323-6. PMID: 17236958.
21. Torcuator R, Zuniga R, Mohan YS et al. Initial experience with bevacizumab treatment for biopsy confirmed cerebral radiation necrosis. *J Neurooncol*. 2009 Aug;94(1):63-8. PMID: 19189055.
22. Levin VA, Bidaut L, Hou P et al. Randomized double-blind placebo-controlled trial of bevacizumab therapy for radiation necrosis of the central nervous system. *Int J Radiat Oncol Biol Phys*. 2011;79(5):1487. PMID: 20399573.

FIGURES

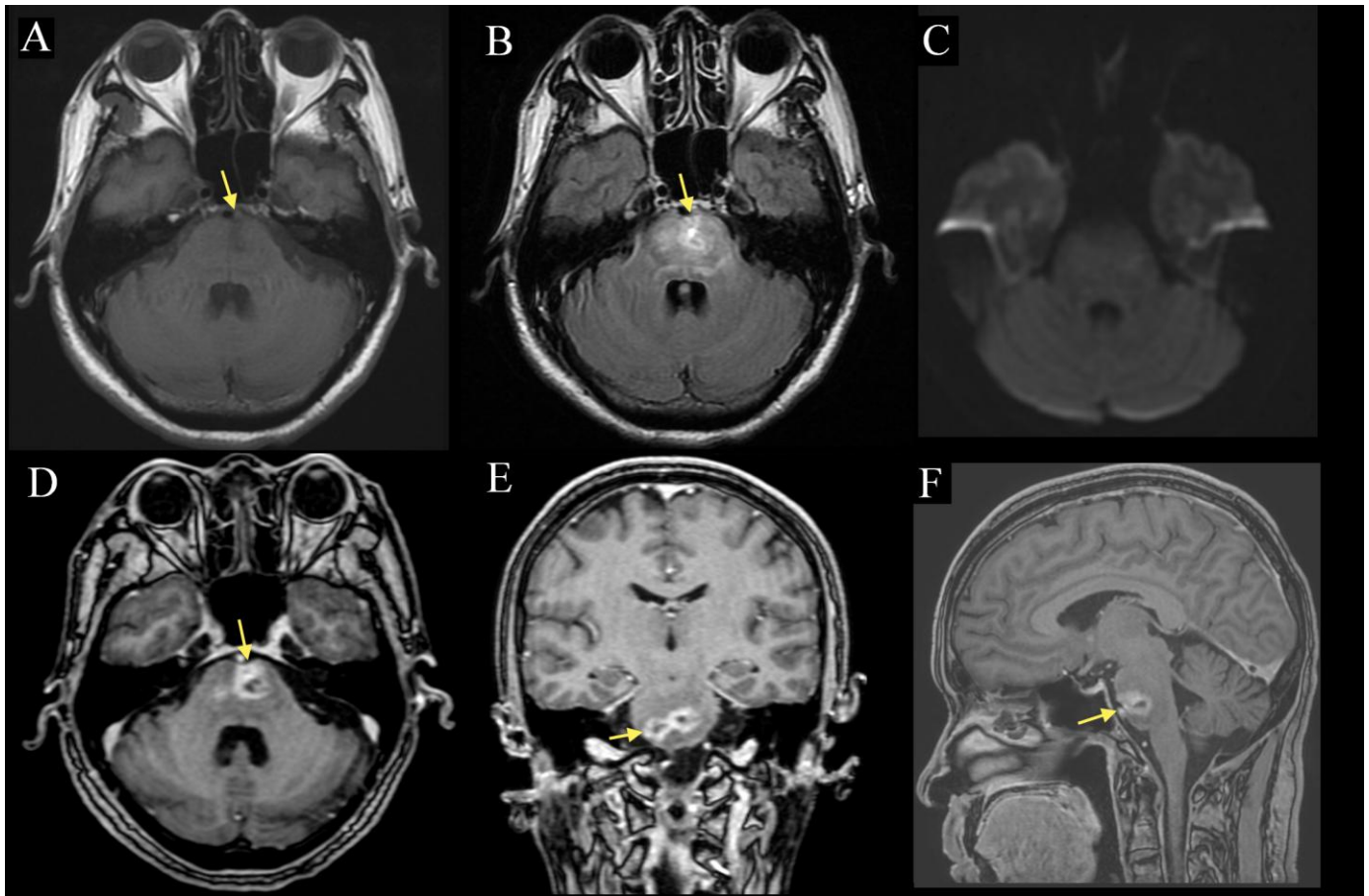


Figure 1: 57-year-old man with radiation necrosis of the pons. Contrast-enhanced MP-RAGE (1D-F) MRI demonstrates two well-circumscribed peripherally contrast-enhancing lesions (arrow) in the pons measuring 14 and 15 mm respectively. The lesions are hypointense on pre-contrast T1 (1A) and are associated with diffuse FLAIR (1B) edema that extends into the medulla and right inferior cerebellar peduncle. There is no obvious mass effect and no extension of the lesion beyond the boundaries of the pons, notably into the cerebellopontine angle or the prepontine cistern. DWI (1C) showed no diffusion abnormality. (A: 1.5 Tesla, TR 400ms, TE 16ms, slice thickness 5.0mm, B: TR 8602ms, TE 129.3ms, slice thickness 5.0mm, C: TR 10000ms, TE 98.3, slice thickness 5.0mm, D: TR 8.4ms, TE 2.6ms, slice thickness 1.6mm. E-F: TR 8.4ms, TE 2.6ms, slice thickness 1.5mm; A-C without contrast, D-F with 10mL of gadopentate dimeglumine (Magnevist))

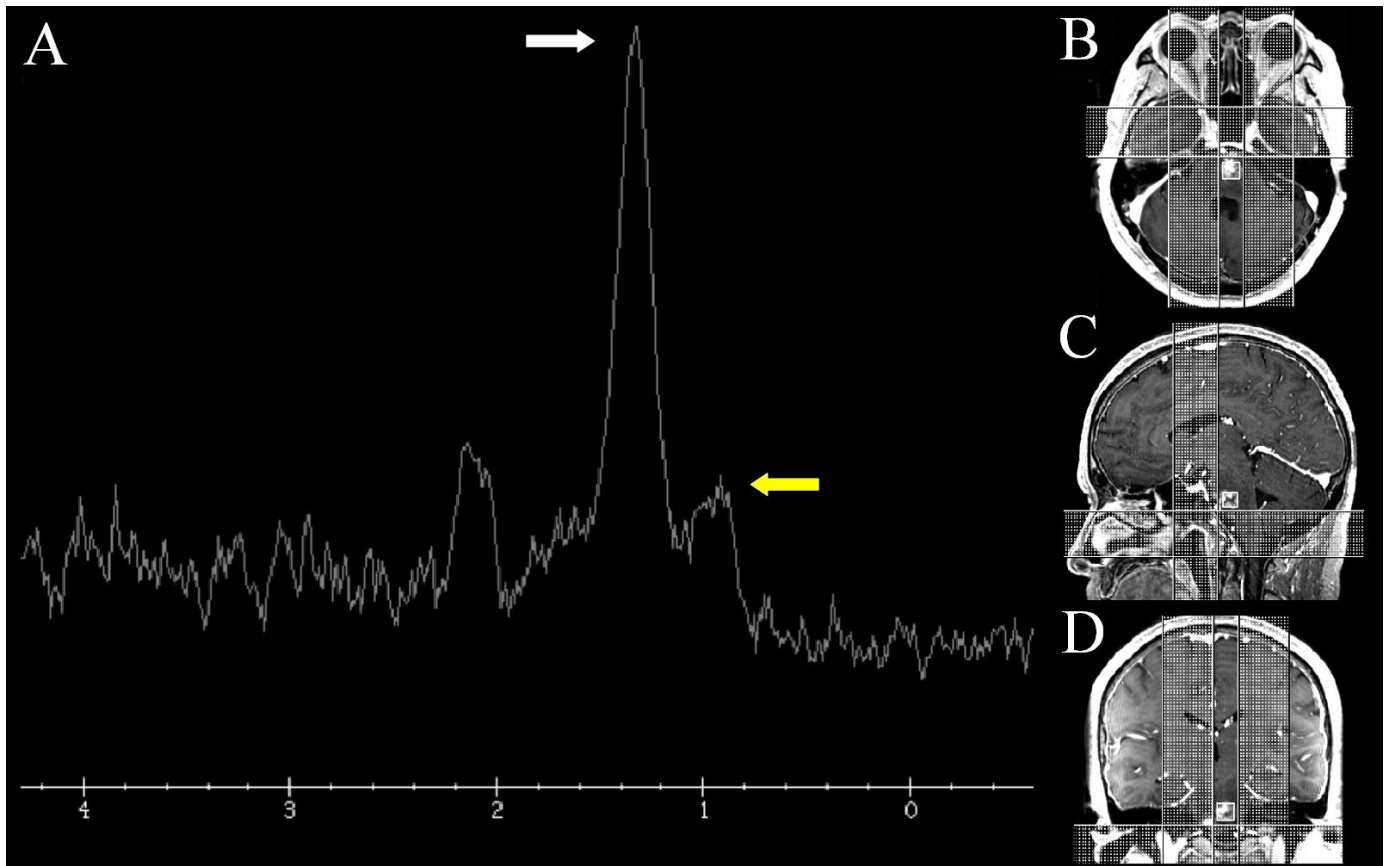


Figure 2: 57-year-old man with radiation necrosis of the pons. Proton MRS (2A) of the pontine lesions (TE 35ms) shows a dominant peak at 1.33ppm (white arrow) and an abnormal peak at 1.0ppm (yellow arrow) representing lactate and lipids respectively. Notably, peaks representing n-acetylaspartate (2.0ppm), choline (3.2ppm) and creatine (3.0ppm) are greatly reduced. Localization (white box) MP-RAGE images (2B-D) taken from the series shown in figure 1D-F. (1.5 Tesla, A: TR 8.4ms, TE 2.6ms, slice thickness 1.6mm. B-C: TR 8.4ms, TE 2.6ms, slice thickness 1.5mm, D: TE 35 ms, A-C 10mL of gadopentate dimeglumine (Magnevist))

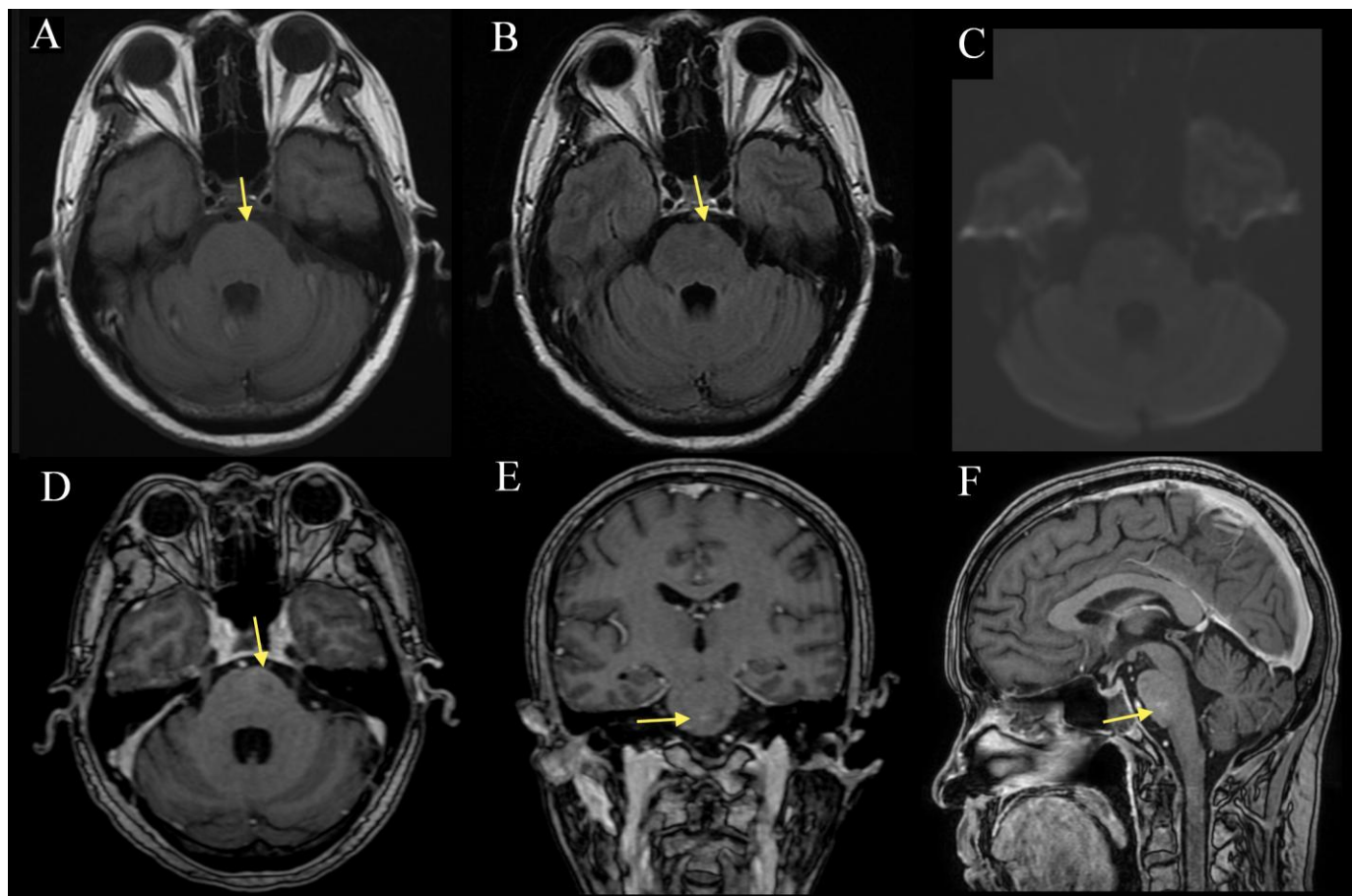


Figure 3: 57-year-old man with radiation necrosis of the pons. Compared to the prior study (figure 1), there is interval size reduction and normalization (arrow) in the T1 (3A) hypointensity, FLAIR (3B) pontine signal abnormality and the associated contrast enhancement on MP-RAGE (3D-F). DWI (3C) continues to show no diffusion abnormality. There is no obvious mass effect of the pontine and cerebellar peduncle lesions and no extension beyond the boundary of the brainstem. (A: 1.5 Tesla, TR 400ms, TE 16ms, slice thickness 5.0mm, B: TR 8602ms, TE 129.4ms, slice thickness 5.0mm, C: TR 10000ms, TE 98.3ms, slice thickness 5.0mm, D: TR 8.4ms, TE 2.6ms, slice thickness 1.6mm. E-F: TR 8.4ms, TE 2.6ms, slice thickness 1.5mm; A-C without contrast, D-F with 13mL of gadopentate dimeglumine (Magnevist))

Etiology	Hypothesized to result from radiation-induced vascular endothelial cell damage, fibrinoid necrosis, microscopic coagulation, demyelination and altered blood-brain barrier permeability.
Incidence	Reported in up to 3% of patients after cranial radiotherapy
Gender Ratio	1:1
Age predilection	Increased incidence with age due to age-related risk of neoplasia and delayed timecourse of lesion development
Risk factors	Cranial radiotherapy
Treatment	Bevacizumab, systemic corticosteroids, surgical decompression, anticoagulation and hyperbaric oxygen
Prognosis	Typically neurological deficits are progressive, however new treatments may slow progression or improve symptoms, though long-term follow-up data is not available.
Magnetic Resonance Imaging	Hypointense T1 signal with hyperintense T2 or FLAIR extending beyond the irradiated area representing edema. Round, irregular, “soap bubble” or “Swiss cheese” appearance. Nodular or peripheral contrast enhancement.
Magnetic Resonance Spectroscopy	Increased lactate and lipid peaks with reduced peaks corresponding to neuro-glial marker such as creatine, n-acetylaspartate and choline.
Nuclear Imaging	Reduced uptake on ¹⁸ F-DG-PET, ¹¹ C-MET PET, ¹²³ IMT SPECT and ²⁰¹ Tl SPECT.

Table 1: Summary table for pontine radiation necrosis

Pontine lesion	MRI T1 signal	MRI T2 signal	Other MRI features	MRS	Nuclear Imaging
Radiation necrosis	Low	High, extending beyond area of irradiation	Round, irregular, "Soap bubble" or "Swiss cheese" appearance. Nodular or peripheral contrast enhancement. Increased diffusion on DWI. Decreased perfusion and blood volume.	Elevated lactate and lipid peaks with reduced NAA, choline, and creatine peaks	Reduced uptake on ¹⁸ FDG-PET, ¹¹ C-MET PET, ¹²³ IMT SPECT and ²⁰¹ Tl SPECT
High-grade glioma	Normal or low	High	Peripheral contrast enhancement (may be uniform in low grade). Increased perfusion and blood volume. Restricted diffusion on DWI.	Lactate may be elevated if necrosis present, decreased NAA and increased choline	Increased uptake on ¹⁸ FDG-PET, ¹¹ C-MET PET, ¹²³ IMT SPECT and ²⁰¹ Tl SPECT
Primary CNS lymphoma	Normal or low	Low, normal or high	Irregular contrast enhancement. Increased perfusion and blood volume. Restricted diffusion on DWI.	Elevated lactate and lipid peaks with decreased NAA and creatine, increased choline	Increased uptake on ¹⁸ FDG-PET, ¹¹ C-MET PET, ¹²³ IMT SPECT and ²⁰¹ Tl SPECT
Toxoplasmosis	Low	Low, normal or high	Nodular or peripheral contrast enhancement. Restricted diffusion on DWI.	Elevated lactate and lipids with absence of other metabolites	Reduced uptake on ¹⁸ FDG-PET, ^{99m} Tc SPECT, ²⁰¹ Tl SPECT and sestamibi SPECT
Listerial/viral rhombencephalitis	Normal or low	High	Patchy, peripheral, gyriform or leptomeningeal contrast enhancement. Increased diffusion on DWI.	Not adequately studied	Reduced uptake on ^{99m} Tc SPECT

Table 2: Differential table for pontine radiation necrosis

ABBREVIATIONS

AIDS = acquired immunodeficiency syndrome
 BBB = blood-brain barrier
 cm = centimeter
 CNS = central nervous system
 CT = computed tomography
 DWI = diffusion-weighted imaging
 FDG = fluorodeoxyglucose
 FLAIR = fluid attenuated inversion recovery
 HIV = human immunodeficiency virus
 HSV = herpes simplex virus
 IMT = iodine-methyltyrosine
 MET = methionine
 mm = millimeter
 MRI = magnetic resonance imaging
 MRS = magnetic resonance spectroscopy
 NAA = n-acetylaspartate
 NPC = nasopharyngeal carcinoma
 PET = positron emission tomography
 SPECT = single photon emission computed tomography
 Tc = technetium
 Tl = thallium
 VEGF = vascular endothelial growth factor

ACKNOWLEDGEMENTS

I would like to thank Veena Venkatachalam for helpful comments and proofreading this report.

Online access

This publication is online available at:
www.radiologycases.com/index.php/radiologycases/article/view/1108

Peer discussion

Discuss this manuscript in our protected discussion forum at:
www.radiopolis.com/forums/JRCR

Interactivity

This publication is available as an interactive article with scroll, window/level, magnify and more features.
 Available online at www.RadiologyCases.com

Published by EduRad



www.EduRad.org

KEYWORDS

Radiation necrosis; pons; nasopharyngeal carcinoma; MR spectroscopy; bevacizumab